

Measurement of quasi-elastic $^{12}\text{C}(p, 2p)$ scattering at high momentum transfer

Y. Mardor¹, J. Aclander¹, J. Alster¹, D. Barton², G. Bunce², A. Carroll², N. Christensen^{3*}, H. Courant³, S. Durrant², S. Gushue², S. Heppelmann⁴, E. Kosonovsky¹, I. Mardor¹, M. Marshak³, Y. Makdisi², E.D. Minor^{4†}, I. Navon¹, H. Nicholson⁵, E. Piassetzky¹, T. Roser², J. Russell⁶, C.S. Sutton⁵, M. Tanaka^{2‡}, C. White³, J-Y Wu^{4§}.

¹*School of Physics and Astronomy, Sackler Faculty of Exact Sciences, Tel Aviv University.* ²*Brookhaven National Laboratory.* ³*Physics Department, University of Minnesota.* ⁴*Physics Department, Pennsylvania State University.* ⁵*Mount Holyoke College.* ⁶*Physics Department, University of Massachusetts Dartmouth.*

We measured the high-momentum quasi-elastic $^{12}\text{C}(p, 2p)$ reaction (at $\theta_{cm} \simeq 90^\circ$ C.M.) for 6 and 7.5 GeV/c incident protons. The three-momentum components of both final state protons were measured and the missing energy and momentum of the target proton in the nucleus were determined.

The validity of the quasi-elastic picture was verified up to Fermi momenta of about 450 MeV/c where it might be questionable. Transverse and longitudinal Fermi momentum distributions of the target proton were measured and compared to independent particle models which do not reproduce the large momentum tails. We also observed that the transverse Fermi distribution gets wider as the longitudinal component increases in the beam direction, in contrast to a simple Fermi gas model.

Quasi-elastic (QE) scattering is a process in which a projectile is elastically scattered from a single bound nucleon in the nucleus, which we call the “target nucleon”, while the rest of the nucleus acts as a spectator. Specifically, the QE (p,2p) scattering at large momentum transfer provides a method for measuring the high momentum tails of the nuclear wave function. This fact can be understood by considering the s-scaling law for high momentum transfer hadronic reactions [1]. The elementary pp elastic differential cross section scales as $d\sigma/dt \sim 1/s^{10}$ for fixed (s/t), where s and t are the Mandelstam variables. Farrar *et al.* [2] pointed out that this scaling will cause the QE (p,2p) reaction in the nucleus to favor

strongly the scattering from those target nucleons that are moving in the beam direction with large Fermi momentum, because the value of s is reduced under those kinematic conditions. The same reaction also attracted much attention in recent years [3] in connection with the QCD prediction that the nuclear attenuation will vanish at asymptotically large momentum transfer, a phenomenon called “Color Transparency” [4]. Thus, at large but finite energies the QE (p,2p) reaction, with emerging protons of a few GeV/c, is a good tool for experimental studies of the nuclear transparency. Those results will be discussed in a forthcoming publication [5].

This letter will concentrate on the identification of QE events and will test the validity of the QE picture up to large Fermi momenta, where it might become questionable. If the QE picture is valid, then over the measured kinematical range it is possible to separate nuclear properties from the nuclear reaction mechanism. We will also present transverse and longitudinal Fermi momentum distributions of the target proton and compare them to independent particle models.

We measured the high-momentum transfer quasi-elastic (p,2p) reaction at $\theta_{cm} \simeq 90^\circ$ on carbon for 6 and 7.5 GeV/c incident protons in a kinematically complete coincidence experiment. The three-momentum components of both high p_t final state protons were measured, which yielded the missing energy and momentum of the target proton in the nucleus.

The experiment (E850) was performed at the AGS accelerator at Brookhaven National Laboratory with the EVA spectrometer [6–8]. The spectrometer consists of a super-conducting solenoidal magnet operated at 0.8 Tesla. The beam enters along the z axis and hits a series of targets located at various z positions. The scattered particles are tracked by four cylindrical chambers (C1–C4). The radii of the cylinders range from 10 to 180 cm. All cylinders and targets can be moved along the solenoid axis in order to optimize the angular acceptance range for each beam momentum. Cylinders C2–C4 have 4 layers of 2 m long straw drift tubes, whose diameters range from 1 cm for C2 to 2 cm for C4. The high resistance central wires are read out at both ends, providing position information along the z direction. Thus, one can extract the z position of the particles in the cylinders as well as their azimuthal angles as they are bent in the axial magnetic field. This provides the transverse momentum of the particles and their scattering angle. The

*Current address: Department of Physics, University of Auckland, New Zealand.

†Current address: “Concurrent Technologies Corporation”, Johnstown, PA, USA.

‡Deceased

§Current address: “Fermi National Accelerator Laboratory”.

1 m long C1 cylinder with a tube diameter of 0.5 cm, was read out at one end only. The readout electronics were designed especially for this spectrometer [9]. The straw tubes were filled with a 50/50 mixture of argon-ethane gas at atmospheric pressure. The drift time measurement from the central wire had a spatial resolution of about 0.3 mm. Three solid targets, CH_2 , C and CD_2 (enriched to 95%) were placed on the z axis inside the C1 cylinder separated by about 20 cm. They were 5.1×5.1 cm^2 squares and 6.6 cm long in the z direction except for the CD_2 target which was 4.9 cm long. Their positions were interchanged at several intervals in order to reduce systematic uncertainties and to maximize the acceptance range for each target.

The spectrometer was located on the secondary line C1 of the AGS. The beam passed through a sequence of two differential Cerenkov counters which identified the incident particles. The beams ranged in intensity from 1 to $2 \cdot 10^7$ over a one second spill every 3 seconds. Two counter hodoscopes in the beam provided beam alignment and a timing reference. Three levels of triggering were used (see ref [10] for a detailed description). The spectrometer included two fan-shaped arrays of scintillator hodoscopes which provided fast triggering of the first level by requiring a minimum transverse momentum. This trigger passed a typical event rate of 100 KHz with a transverse momentum cut-off resolution of about 7%. The second level trigger selected high transverse momentum particles with a 4% momentum resolution and accepted a rate of 10 KHz. The third level trigger allowed a wide range of choices for the angles of the two fast particles. The accepted rate ranged from 10 to 40/sec.

The coordinate system was chosen with the z coordinate in the beam direction and the y direction normal to the scattering plane (x, z). The latter is defined by the incident beam and either one of the emerging protons. The data were analyzed in terms of the momenta in the y direction (P_{fy}) and the light cone variable $\alpha = (E_f - P_{fz})/m$, where E_f is the total target nucleon energy, P_{fz} is the z component of the target proton momentum and m is the mass of the target proton. The variable α is a natural choice for high energy reactions and is also ideally adapted to our experimental analysis. We determined α with a precision of $\sigma \simeq 3\%$. Setting $E_f \simeq m$, we can write $\alpha \simeq 1 - P_{fz}/m$, and with the additional good approximation in our kinematical region $E_0 = P_0$, we can write:

$$s \sim m^2 + \tilde{m}^2 + 2mP_0\alpha \quad (1)$$

where E_0 and P_0 are the energy and momentum of the incident proton and \tilde{m} is the off-mass-shell mass of the target nucleon. Setting $\tilde{m} \simeq m$:

$$s \sim 2m^2 + 2mP_0\alpha \quad (2)$$

This makes s proportional to α . The P_{fy} had a resolution of $\sigma = 40$ MeV/c and the resolution in P_{fx} was

$\sigma = 170$ MeV/c. Because of its better resolution, P_{fy} was used to represent a transverse component. Both the α and P_{fy} resolutions were determined by the elastic pp scattering events from the CH_2 target.

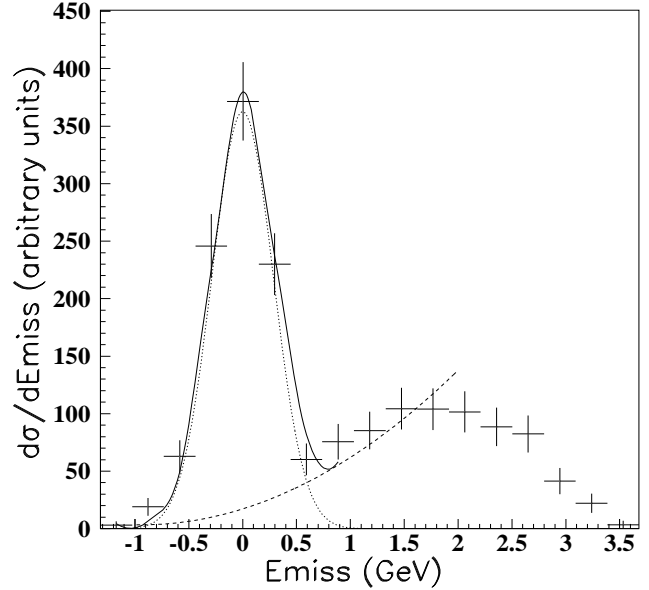


FIG. 1. E_{miss} distribution for 6 GeV/c, $0.1 < |P_{fy}| < 0.2$ GeV/c, and $|\alpha - 0.87| < 0.05$. The Gaussian (dotted line) represents the QE events. The shape of the background (dashed curve) was deduced from extra track events. The fall-off above 1.5 GeV is an artifact of the trigger. The solid curve is the result of the fit (see text).

The quasi-elastic scattering nature was ensured by selecting events from the C target with just two tracks in the detector and by software cuts on the quality of track reconstruction. An upper limit on the excitation energy of the residual nucleus (E_{miss}) was imposed in order to eliminate events where additional particles could be produced. Given our resolution for E_{miss} , we applied a cut of $|E_{miss}| < 0.5$ GeV. Since this cut is above m_π , some inelastic background from soft neutral particles, such as those coming from $pA \rightarrow pp\pi^0(A-1)$ events, could penetrate the cuts and had to be subtracted. The shape of this background was determined from a fit to the E_{miss} distribution of events with extra tracks in the spectrometer. Subsequently, we used that shape to fit the E_{miss} spectrum for 50 MeV/c wide P_{fy} bins to the background (BG) and a Gaussian centered at $E_{miss} \simeq 0$ which represents the QE events. The width of the Gaussian was determined from a fit to the peak at $E_{miss} \simeq 0$ for $0 < P_{fy} < 50$ MeV/c, where the peak is very prominent. The reported α and P_{fy} distributions are the results of these fits. An example is shown in Figure 1.

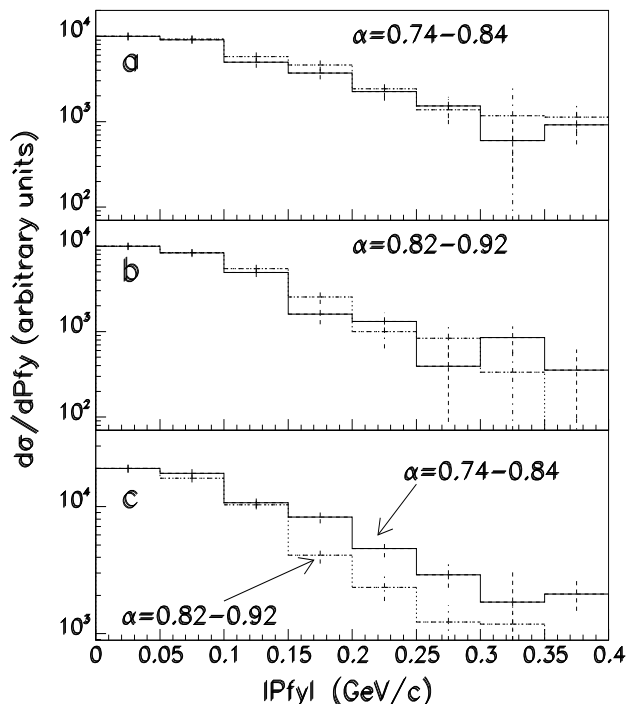


FIG. 2. a-b: $|P_{fy}|$ distributions for different α slices. The 6 GeV/c (solid line) and the 7.5 GeV/c (dashed line) distributions were normalized at $P_{fy} = 0$. c: $|P_{fy}|$ distributions for $\alpha = 0.79$ (solid line) and for $\alpha = 0.87$ (dashed line). The data in each α range are summed for 6 and 7.5 GeV/c (see text). The two distributions were normalized at $P_{fy} = 0$.

In Figure 2 we present $|P_{fy}|$ distributions. Figs. 2(a)-2(b) show the P_{fy} distributions for two regions of α , at 6 and 7.5 GeV/c. The curves were normalized at $P_{fy} = 0$ and we see that the shapes are independent of the incident energy within the experimental errors. This is what one expects from the impulse approximation (IA). In the IA the QE cross section is factorized into contributions from the probability to find a nucleon with Fermi momentum \vec{P}_f in the nucleus $n(P_{fz}, \vec{P}_{ft})$, the free pp elastic cross section and the nuclear transparency $T(s, t)$:

$$\frac{d^3\sigma}{d\vec{P}_f}(s, t)_{q.e.} = \int \frac{d\sigma}{dt}(s, t)_{free} \cdot n(P_{fz}, \vec{P}_{ft}) \cdot T(s, t) dt \quad (3)$$

For scattering at $\theta_{cm} \simeq 90^\circ$ the free cross section is a function of s only. For a narrow region of α corresponding to a narrow region of s , we can then write:

$$\frac{d^2\sigma}{d\vec{P}_{ft}}(\alpha)_{q.e.} = n(\vec{P}_{ft}) \cdot Factor(\alpha) \quad (4)$$

This means that for fixed α , the $|P_{fy}|$ distributions at the two incident energies will scale by some function of s

as can be seen clearly in Figure 2. Note that for small α (Fig. 2(b)) the P_{fz} is about 200 MeV/c and, since the scaling holds also for large P_{fy} , the scaling has been checked up to a fairly large Fermi momentum (about 0.5 GeV/c).

In Fig. 2(c) we compare the transverse Fermi distributions for two different α ranges. Since the shapes were shown to be independent of the incident energies we summed the measured distributions for the two incident energies. We observe that the transverse Fermi distribution gets wider for larger longitudinal Fermi momentum distributions (smaller α). This is in contradiction to what one would expect from a simple Fermi gas model. With a given distribution $|P_f|$, a large P_{fz} would give a narrower P_{fy} distribution.

As we mentioned in the introduction, the large momentum transfer QE ($p, 2p$) reaction prefers small s (small α) due to the strong s dependence of the elementary pp elastic cross section. The flux factor for the quasi-elastic pp cross section is different from the free pp one, due to the motion of the target proton in the nucleus. Since the differential cross section is not invariant, there are also Jacobians that have to be included when changing reference frames. Taking these effects into account, we obtained the nuclear momentum distribution, $n(P_{fz})$, by multiplying the measured α distribution, $\frac{\Delta N}{\Delta\alpha}$, by the factor of Equation 5:

$$n(P_{fz}) \propto \frac{\Delta N}{\Delta\alpha} \left(\frac{E_2 - P_{2z}}{mP_1} \frac{1}{s(s - 4m^2) \left(\frac{d\sigma}{dt} \right)_{pp}} \right)_{P_{1t} = -P_{2t}} \quad (5)$$

where $\frac{d\sigma}{dt}_{pp}$ is the measured free pp cross section [11], P_1 is the momentum of one of the outgoing protons, E_2 and P_{2z} are the energy and z momentum component of the other one, and P_{1t} and P_{2t} are the transverse components of the two outgoing particles. A derivation of the factor is given elsewhere [8].

After this correction the two measured α distributions at 6 and 7.5 GeV/c were consistent with each other in shape, so we joined the two sets of measurements. The result is shown in Figure 3 which, up to distortion from initial and final state interactions, represents the P_{fz} distribution of the target nucleon.

The transverse distribution (P_{fy}), shown in Figure 3, was obtained by adding the measured distributions of the measured α regions, weighted according to the integrated number of events in the measured α distribution. We see that the longitudinal and the transverse distributions have the same shape in spite of the very different procedures used to get them.

Also in Figure 3, the data are compared to a prediction of a simple independent particle Fermi motion distribution. An harmonic oscillator model (HO) was used with parameters fitted to ^{12}C from electron scattering with

the kinematical constraints of our measurement [12]. As can be seen clearly, the independent particle model fails substantially to describe the large momentum tails of the distribution. In order to quantify this statement, we present the ratio between the number of events with $154 < P_{fz} < 280$ MeV/c and the number of events with $0 < P_{fz} < 154$ MeV/c (we measured events with $P_{fz} > 0$ and we assumed that the distribution is symmetric about $P_{fz} = 0$). The measured ratio is $(29 \pm 2)\%$. The HO prediction for the same ratio is only 11.7%.

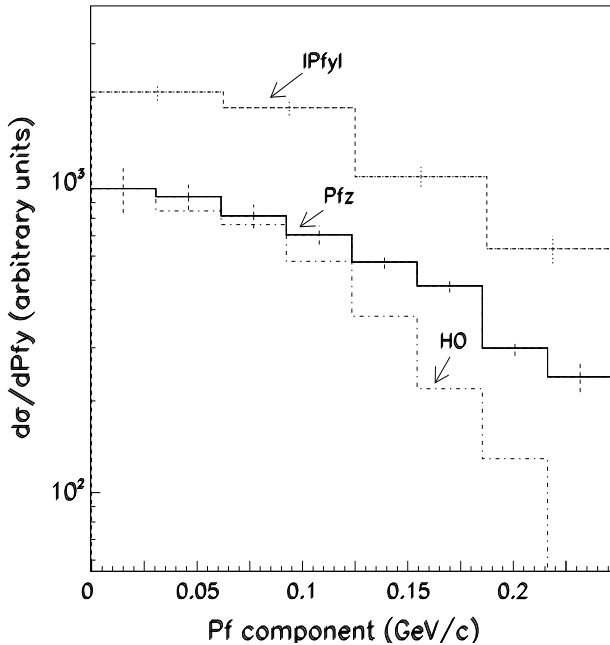


FIG. 3. P_{fz} is the longitudinal momentum distribution, obtained from the α distributions measured at 6 and 7.5 GeV/c and corrected for the s dependence induced by the elementary free cross section. $|P_{fy}|$ is the transverse distribution, obtained from the measured transverse distributions, at several α regions (see text). HO is a harmonic oscillator independent particle model calculation. The P_{fz} and HO distributions are normalized to 1000 at the first bin.

In conclusion, the QE events were identified and we showed that it is possible to separate the nuclear properties (Fermi momentum distribution) from the reaction mechanism up to a total Fermi momentum of about 0.5 GeV/c. Based on this result, we deduced transverse and longitudinal Fermi distributions up to large momenta. The tails of these distributions are consistent with electron scattering data [13] and are larger than predicted by independent particle models and are characteristic for short range correlation. We also found that the transverse Fermi distribution increases as P_{fz} increases.

Very special thanks are due to Dr. M.Sargsyan, who accompanied our analysis with detailed calculations. We

wish to thank Drs. L. Frankfurt, M. Strikman, G. Miller for their theoretical input. S. Baker, F.J. Barbosa, S. Kaye, M. Kmit, D. Martel, D. Maxam, J.E. Passaneau, M. Zilca contributed significantly to the design and construction of the detector.

We are pleased to acknowledge the assistance of the AGS staff in building the detector and supporting the experiment, particularly our liaison engineers, J. Mills, D. Dayton, C. Pearson. We acknowledge the continuing support of D. Lowenstein and P. Pile.

This research was supported by the U.S - Israel Binational Science Foundation, the Israel Science Foundation founded by the Israel Academy of Sciences and Humanities, NSF grant PHY-9501114 and Department of Energy grants DEFG0290 ER40553.

-
- [1] S.J. Brodsky and G.R. Farrar, Phys. Rev. Lett. 31, 1153 (1973).
 - [2] G.R. Farrar *et al.*, Phys. Rev. Lett. 62, 1095 (1989)
 - [3] A.S. Carroll *et al.*, Phys. Rev. Lett. 61, 1698 (1988); S. Heppelmann *et al.*, Phys. Let. B232, 167 (1989).
 - [4] A. Mueller, in: *Proc. XVII Rencontres de Moriond* (Les Arcs, France, 1982), ed. by J. Tran Thanh Van (Editions Frontieres, Gif-sur-Yvette, 1982) p.13. S.J. Brodsky, in: *Proc. XIII Intern. Symp. on Multi-particle Dynamics*, ed. by E.W. Kittel, W. Metzger, and A. Stergiou (World Scientific, Singapore, 1982) p. 963. P. Jain, J.P. Ralston and B. Pire, Review
 - [5] S. Durrant *et al.* In preparation.
 - [6] M. A. Shupe *et al.* EVA, a solenoidal detector for large angle exclusive reactions: Phase I - determining color transparency to 22 GeV/c. Experiment E850 Proposal to Brookhaven National Laboratory, 1988 (unpublished).
 - [7] *Measurement of the dependence of the $C(p, 2p)$ cross section on the transverse component of the spectral momentum*, S. Durrant, PhD Thesis, Pennsylvania State University, 1994 (unpublished).
 - [8] *Quasi-Elastic Hadronic Scattering at Large Momentum Transfer*, Y. Mardor, PhD Thesis, Tel Aviv University, 1997 (unpublished).
 - [9] *EVA Straw Tube Electronics, EXP850, BNL*, Fernando J. Barbosa. 1991 (unpublished).
 - [10] *The EVA Trigger: Transverse momentum selection in a solenoid*, J.Y. Wu *et al.*, Nuclear Instruments and Methods A 349 (1994) 183-196.
 - [11] *Compilation of Nucleon - Nucleon and Nucleon - Antinucleon Elastic Scattering Data*. M.K. Carter, P.D.B. Collins and M.R. Whalley. Rutherford Lab. publication PAL-86-002 (1986).
 - [12] M. Sargsyan, Private Communication; H. Bidasaria, P.M. Fishbane and J.V. Noble, Nucl. Phys. A355, 349 (1981).
 - [13] D. Day *et al.*, Phys. Rev. Lett. 38, 259 (1982).